Development 138, 4001-4012 (2011) doi:10.1242/dev.065003

Loss of MAP3K1 enhances proliferation and apoptosis during retinal development

Maureen Mongan[1], Jingcai Wang[1,2], Hongshan Liu[3], Yunxia Fan[1], Chang Jin[1], Winston Y.-W. Kao[3] and Ying Xia[1,3,*]

SUMMARY

Precise coordination of progenitor cell proliferation and differentiation is essential for proper organ morphogenesis and function during mammalian development. The mitogen-activated protein kinase kinase kinase 1 (MAP3K1) has a well-established role in anterior eyelid development, as *Map3k1*-knockout mice have defective embryonic eyelid closure and an 'eye-open at birth' (EOB) phenotype. Here, we show that MAP3K1 is highly expressed in the posterior of the developing eye and is required for retina development. The MAP3K1-deficient mice exhibit increased proliferation and apoptosis, and Müller glial cell overproduction in the developing retinas. Consequently, the retinas of these mice show localized rosette-like arrangements in the outer nuclear layer, and develop abnormal vascularization, broken down retinal pigment epithelium, photoreceptor loss and early onset of retinal degeneration. Although the retinal defect is associated with increased cyclin D1 and CDK4/6 expression, and RB phosphorylation and E2F-target gene upregulation, it is independent of the EOB phenotype and of JNK. The retinal developmental defect still occurs in knockout mice that have undergone tarsorrhaphy, but is absent in compound mutant *Map3k1*$^{+/\Delta KD}$*Jnk1*$^{-/-}$ and *Map3k1*$^{+/\Delta KD}$*Jnk*$^{+/-}$*Jnk2*$^{+/-}$ mice that have EOB and reduced JNK signaling. Our results unveil a novel role for MAP3K1 in which it crosstalks with the cell cycle regulatory pathways in the prevention of retina malformation and degeneration.

KEY WORDS: MAP3K1, Retina development, E2F, Mouse

INTRODUCTION

MAP3K1 is a member of the mitogen-activated protein kinase kinase kinase (MAP3K) superfamily, the members of which are known to have highly cell type-specific roles in the control of MAPKK-MAPK signaling cascades. In vivo studies using mice that lack either the full-length protein (MAP3K1 null or *Map3k1*$^{-/-}$) or the kinase domain (*Map3k1*$^{\Delta KD/\Delta KD}$) have revealed essential roles of this protein kinase in the regulation of immune system development and function (Gallagher et al., 2007; Gao et al., 2004; Labuda et al., 2006; Venuprasad et al., 2006), injury repair (Deng et al., 2006; Mongan et al., 2008), vasculature remodeling (Li et al., 2005), and tumor progression (Cuevas et al., 2006). Yet, the most apparent function of MAP3K1 is the regulation of ocular surface morphogenesis. Although both *Map3k1*$^{\Delta KD/\Delta KD}$ and MAP3K1-null mice survive embryonic development, they display a distinct eye open at birth (EOB) phenotype, owing to defective eyelid morphogenesis (Yujiri et al., 1998; Zhang et al., 2003). Detailed characterization of the knockout mice indicates that MAP3K1 is responsible for transmission of morphogenic signals to the activation of a JNK-c-Jun pathway, which is required for induction of actin polymerization and expression of genes involved in epithelial cell migration (Deng et al., 2006; Zhang et al., 2003; Zhang et al., 2005). Thus, loss of MAP3K1 impairs epithelial cell migration and thereby embryonic eyelid closure.

In addition to the EOB phenotype, MAP3K1-deficient mice display numerous eye abnormalities at postnatal ages. In the anterior segment, they show eyelid attachment to the cornea, iris pigment cell outgrowth, corneal inflammation and morphological abnormalities. In the posterior segment, *Map3k1*$^{\Delta KD/\Delta KD}$ mice display a distinct retinal dysplasia (Zhang et al., 2003). Although the anterior pathologies may be secondary to EOB, as lacking a closed eyelid exposes the premature ocular surface to environmental insults that may cause injury, the posterior defects are more likely to be attributed to MAP3K1 deficiency. How MAP3K1 regulates retina development, however, has not been explored.

The retina is a part of the central nervous system that lines the back of the eye, with a function in capture and conversion of light particles into nerve signals. The mature retina consists of three nuclear layers and seven major cell types (Livesey and Cepko, 2001). The outer nuclear layer (ONL) contains cell bodies of photoreceptors, rods and cones, which are the light-detecting neurons of the eye. The inner nuclear layer (INL) consists of horizontal, bipolar, amacrine interneuron and Müller glia, whereas the innermost ganglion cell layer (GCL) consists of ganglion and amacrine neurons, which are responsible for processing the visual signals that are sent through the optical nerve to the brain. All these cells derive from the multipotent retinal progenitor cells (RPCs) in a temporal and overlapping period of time during development (Chen et al., 2004; Chow and Lang, 2001). The RPCs have the ability to proliferate in order to produce enough cells for the growing retina. This takes place in mouse in a 17-day period between embryonic day (E) 14 and postnatal day (P) 8. Concurrently, subpopulations of RPCs will commit to precursors at the appropriate developmental stage, whereas the committed precursors will stop proliferation and exit the cell-cycle through an intrinsic program (Zhang et al., 2004).

[1]Department of Environmental Health, University of Cincinnati, College of Medicine, Cincinnati, OH 45267-0056, USA. [2]Department of Histology and Embryology, Southern Medical University, Guangzhou, China. [3]Department of Ophthalmology, University of Cincinnati, College of Medicine, Cincinnati, OH 45267-0056, USA.

*Author for correspondence (ying.xia@uc.edu)

Accepted 5 July 2011

Precise coordination of proliferation and differentiation is essential for retina development, whereas its disruption leads to retina malformation.

Genetic studies in mice have shown that loss of the retinoblastoma gene *Rb* uncouples cell cycle exit from differentiation, resulting in extended precursor proliferation and pathological lesions in the retina (Ajioka and Dyer, 2008; Chen et al., 2004; MacPherson et al., 2004). The RB-deficient retinas also display increased apoptosis, which is likely to be a compensatory mechanism to minimize visual impairment, so that RB knockout mice rarely develop invasive retinoblastoma. RB is a nuclear phosphoprotein that controls the cell cycle by binding to members of the E2F family of transcription factors, resulting in repression of E2F1-mediated gene expression (Hatakeyama and Weinberg, 1995; Polager and Ginsberg, 2009; Stevaux and Dyson, 2002). Inactivation of RB is accomplished by gene mutation or cyclin-dependent kinases-mediated RB phosphorylation that dissolves the RB/E2F complex, which leads to E2F activation. The E2F in turn regulates genes whose products are implicated in the G1- to S-phase transition of cell cycle, in DNA replication and in apoptosis (Iaquinta and Lees, 2007; Rowland and Bernards, 2006). Genetic deletion of E2F1 rescues abnormalities in ectopic division and apoptosis of RB-deficient retinal cells, supporting the existence of a RB-E2F axis in retinal development (Chen et al., 2007).

It is generally accepted that extrinsic signals play important roles in establishing the correct balance between RPC proliferation and precursor generation during development. The growth factor-stimulated signaling pathways, such as the MAPK cascades, have been shown to modulate RB and E2F activities in the context of cell cycle progression of cancer (Downward, 1997), but their interactions with the RB-E2F axis in retina development have not been well understood (Oliveira et al., 2008). In this paper, we focused on investigating the role of MAP3K1 in retina development. We show that MAP3K1 is highly expressed in the postnatal retina and its ablation leads to activation of the RB/E2F pathways. Consequently, the MAP3K1-deficient retina displays aberrant proliferation, apoptosis and Müller glia overproduction, leading to abnormal retinal structure and early onset of retinal degeneration. The retinal defects in the MAP3K1-null mice are not due to reduction of JNK activation and open eyelids. Results of this work reveal a novel JNK-independent function of MAP3K1 in the regulation of cell proliferation and differentiation.

MATERIALS AND METHODS

Reagents and antibodies

The antibodies for F4/80 were from Abcam (Cambridge, MA, USA), PCNA was from BD Biosciences (Bedford, MA, USA), p-JNK was from Promega (Madison, WI, USA), and p-H3, rhodopsin and opsin blue were from Millipore (Bedford, MA, USA). Antibodies for glutamine synthetase, calbindin-D-28K, protein kinase C, the Harris Hematoxylin solution and alcoholic Eosin Y solution were from Sigma (St Louis, MO, USA). Anti-p-RB was from Santa Cruz Biotechnology (Santa Cruz, CA, USA). The Alexa Fluor-conjugated secondary antibody, random hexamer primers and the enzyme for reverse transcription were from Invitrogen (Carlsbad, CA, USA). The ApopTag Plus fluorescent in situ apoptosis detection kit for TUNEL assays was from Chemicon (Billerica, MA, USA). The TRIzol reagents for RNA isolation were from QIAGEN (Valencia, CA, USA) and SYBER Green QPCR Master Mix was from Stratagene (Santa Clara, CA, USA).

Experimental animals

The wild-type, *Map3k1*$^{+/\Delta KD}$, *Map3k1*$^{\Delta KD/\Delta KD}$, *Map3k1*$^{+/\Delta KD}$*Jnk1*$^{-/-}$ and *Map3k1*$^{+/\Delta KD}$*Jnk*$^{+/-}$*Jnk2*$^{+/-}$ mice were generated by standard mating strategies as described previously (Takatori et al., 2008; Zhang et al., 2003). The *Map3k1*$^{+/\Delta KD}$ mice were backcrossed to the CD-1 mouse strain purchased from the Jackson Laboratory (Maine, USA) to produce albino *Map3k1*$^{+/\Delta KD}$ and *Map3k1*$^{\Delta KD/\Delta KD}$ mice. In some experiments, eyelid surgical procedures were applied to wild-type and *Map3k1*$^{\Delta KD/\Delta KD}$ mice at P0. Specifically, the eyelids of the *Map3k1*$^{\Delta KD/\Delta KD}$ mice were sutured with sterile non-absorbable surgical suture u.s.p. 10-0 (Alcon, Fort Worth, TX, USA) and the suture was removed at P14. The eyelids of wild-type mice at P0 were surgically separated at the upper and lower lid fusion line. The pups were raised by the mother until P15. All experiments conducted have been approved by the University of Cincinnati Animal Care and Use Committee.

Histology, β-galactosidase staining, immunohistochemistry and the TUNEL assays

The whole mount β-gal staining was carried out as described before (Henkemeyer et al., 1996). Briefly, the mouse eyes were enucleated, fixed in cold 2% paraformaldehyde plus 0.25% glutaraldehyde for 15 minutes. The tissues were washed in PBS and placed in X-gal staining solution at 37°C overnight. For histology and immunohistochemistry, the mouse eyes were fixed in 4% paraformaldehyde at 4°C overnight. The eyes were embedded in paraffin and sectioned, and eye sections were counterstained with Hematoxylin and Eosin or subjected to immunostaining. Immunostaining was done using specific antibodies followed by Alexa Fluor dye-conjugated secondary antibodies and Hoechst to label nuclei.

Tissue sections were applied to TUNEL assay following the protocol from the supplier. Briefly, the paraffin sections were deparaffinized and incubated with TdT enzyme. The sections were then incubated with anti-digoxigenin-fluorescein conjugates, followed by staining with Hoechst. The tissue sections were examined and photographed using a Zeiss Axiocam microscope (Carl Zeiss, Thornwood, NY, USA).

RNA isolation, reverse transcription and real time PCR

Retinas were isolated under a dissecting microscope (Nikon, Melville, NY, USA) from the mice at P5 of age. Total RNA was extracted using TRIzol reagents and was reverse transcribed to generate cDNA using a kit from Invitrogen. Quantitative PCR was performed using an MX3000p thermal cycler system and SYBER Green QPCR Master Mix. At the end of the PCR, the samples were subjected to melting curve analysis. All reactions were performed at least three times in four biological samples. Relative differences in QRT-PCR among samples were determined using the $\Delta\Delta C_t$ method as described previously (Peng et al., 2007). Oligonucleotides used as the specific primers to amplify mouse genes cDNA were as follows: exons of MAPK kinase domain, 5′-CCGCCATCCACTCAATGAAGA CG and 5′-CCAAAGCGAAACAGCCTTACAGAG; *E2f1*, 5′-CTGCCT-CATTGGAATAGCAC and 5′-ACATACACACACACACACAC; *Polα*, 5′-ACGCTCCAGACGCGCACTAC and 5′-TTGGAACGGGA-AGCGGAAG; *Dhfr*, 5′-AGCCTTAGCTGCACAAATAG and 5′-TCTC-CGTTCTTGCCAATCC; cyclin A2 (*Ccna2*), 5′-TACCTGCCTTCACT-CATTGCTGGA and 5′-ATTGACTGTTGGGCATGTTGTGGC; cyclin E1 (*Ccne1*), 5′-TGGATTTGCTGGACAAAGCCCAAG and 5′-AG-GCAATGGCAGGTTTGGTCATTC; *Rb1*, 5′-GACAGCTTCCCCCA-TTTCTTC and 5′-CTTGAACTCACTAGCAAAAGACC; cyclin D1 (*Ccnd1*), 5′-GCCCTCCGTATCTTACTTCAAG and 5′-GCG-GTCCAGGTAGTTCATG; *Cdk4*, 5′-ATCGGGACATCAAGGTCAC and 5′-GTCAGCATTTCCAGTAGCAG; *Cdk6*, 5′-CCCAACGTGGTC-AGGTTGTTTGAT and 5′-AGCCAGCTTTATCTGTCCACTGCT.

Quantification and statistical analyses

The number of p-JNK, p-H3 and TUNEL-positive cells was counted in the photographs that cover the entire retinal cross-section. The average of positive cells per retina was generated based on data from at least eight retinas per genotype in each developmental stage. The number of PCNA-positive and total cells was counted in the photographed field of the retinas. The percentage of PCNA-positive cells was calculated based on four pictures per retina and five retinas per genotype in each developmental stage.

The AxioVision software by Carl Zeiss Imaging was used to measure the thickness of the ONL or INL and the fluorescence density of a standard area across a 5 μm section of retina at 20× magnification. The average of

five pictures per retina and six retinas per genotype was calculated. Statistical comparisons were performed with Student's two-tailed paired *t*-test and analysis of variance (ANOVA). Values of $*P<0.05$, $**P<0.01$ and $***P<0.001$ were considered to be statistically significant.

RESULTS

MAP3K1 expression in postnatal retina

The MAP3Ks display tissue and cell type specificity in signal transduction, partly owing to its unique tissue distribution (Schlesinger et al., 1998). To determine whether MAP3K1 was involved in the postnatal development of eye, particularly retina, we examined its expression in *Map3k1*$^{+/\Delta KD}$ and *Map3k1*$^{\Delta KD/\Delta KD}$ mice. The *Map3k1*$^{\Delta KD}$ allele was generated by replacing exons coding for the kinase domain of MAP3K1 with a β-galactosidase gene such that the resultant MAP3K1ΔC-β-GAL fusion protein was kinase inactive (Xia et al., 2000). Whole-mount X-gal staining of eyes at postnatal day 1 (P1) and P7 showed that the β-gal-positive, i.e. MAP3K1-expressing, cells were abundant in distinct regions of the eye in the *Map3k1*$^{\Delta KD/\Delta KD}$ and less so in *Map3k1*$^{+/\Delta KD}$ mice. By contrast, β-gal-positive cells were undetectable in wild-type mice.

Examination of the eye sections revealed that MAP3K1 was expressed in ectodermal-derived epithelial cells, in agreement with our previous findings in other tissues (Mongan et al., 2008; Zhang et al., 2003). In the anterior eyes, MAP3K1 expression was strong in the epithelium of eyelid, lens and ciliary body, but was weak in corneal epithelial cells, and in corneal and eyelid stromal cells (Fig. 1A,B). In the posterior eyes, MAP3K1 expression was detected broadly in the developing retinas, with particularly high expression in cells occupying the outer neuroblast layer. Although β-gal-positive cells were sparsely seen in the retinal pigment epithelium (RPE) of C57/BL6 mice, they were clearly observed in the RPE of albino CD1 mice (Fig. 1B). Given that the available MAP3K1 antibodies are not qualified for immunostaining, we use β-gal staining as surrogates to show that MAP3K1 is expressed in multiple cell types in anterior and posterior segments of the developing eye.

To confirm MAP3K1 expression, we isolated RNA from retinas of wild-type and *Map3k1*$^{\Delta KD/\Delta KD}$ mice at different postnatal ages. The RNA was analyzed by real-time PCR using primers that recognize the exons coding for the kinase domain of MAP3K1. Although *Map3k1* expression was at background levels in the knockout retinas, it was 20-140 times higher in retinas of age-matched wild-type mice (Fig. 1C). The abundant MAP3K1 expression in the developing retina hints at the possibility that MAP3K1 has a role in postnatal retina development and function.

MAP3K1 is essential for postnatal retinal development

To evaluate whether MAP3K1 was required for retina development, we examined the *Map3k1*$^{+/\Delta KD}$ and *Map3k1*$^{\Delta KD/\Delta KD}$ retinas at different postnatal stages. In contrast to the *Map3k1*$^{+/\Delta KD}$ mice that had normal retinas, the majority (over 95%) of the *Map3k1*$^{\Delta KD/\Delta KD}$ mice had clear retinal abnormalities (Fig. 2A). At early (P1-P6) stage, the retinas of the *Map3k1*$^{\Delta KD/\Delta KD}$ were not much different from those of the *Map3k1*$^{+/\Delta KD}$ mice, both were composed of a layer of RPCs that were not yet fully differentiated.

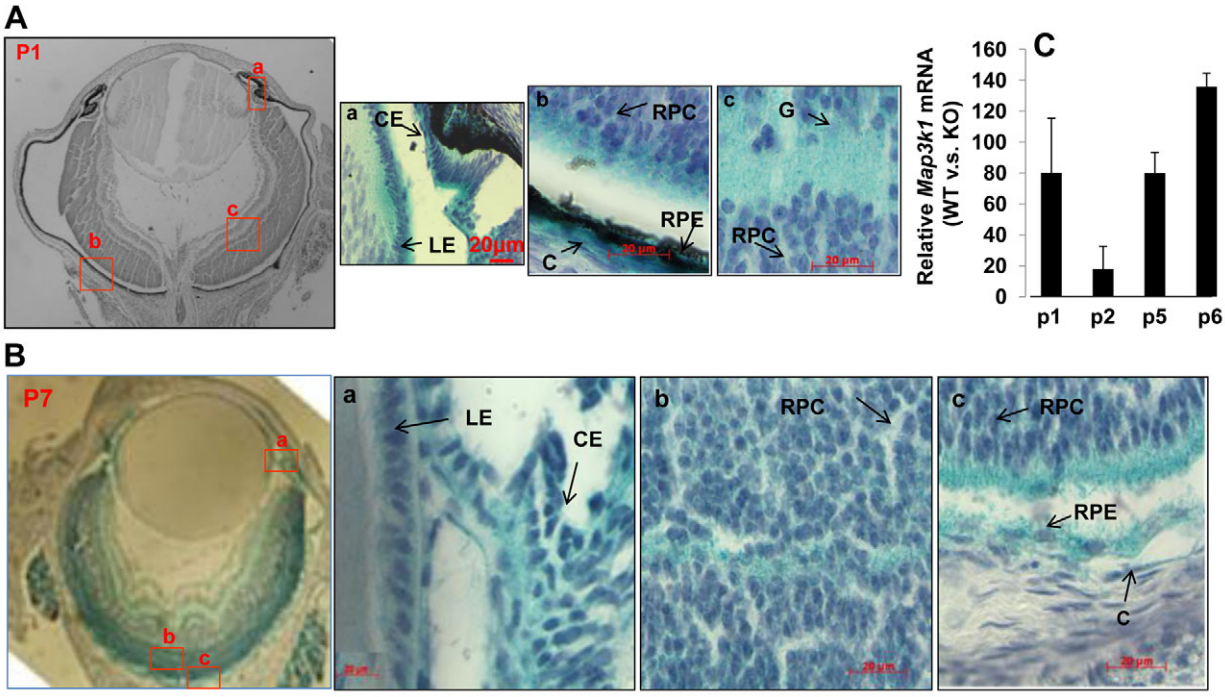

Fig. 1. MAP3K1 expression in the developing eye. (**A**,**B**) Eyes isolated from the *Map3k1*$^{+/\Delta KD}$ mice at (A) P1 and (B) P7 were subjected to whole mount X-gal staining and the histological sections were examined and photographed under a microscope. Arrows indicate the areas where the specific cell types are located. LE, lens epithelium; CE, ciliary epithelium; RPC, retinal progenitor cells; G, ganglion cells; RPE, retinal pigment epithelial cells; C, choroid. Scale bars: 20 μm. (**C**) RNA isolated from the retinas of wild-type and *Map3k1*$^{\Delta KD/\Delta KD}$ mice at different postnatal ages was subjected to real-time RT-PCR for *Map3k1* expression. The levels of MAP3K1 in the knockout mice were similar to that in the control (no RNA) samples. In each age group, the expression of MAP3K1 in wild-type mice was compared with that in *Map3k1*$^{\Delta KD/\Delta KD}$ mice, set as 1. The results represent average of four samples at each genotype/age group+s.e.m.

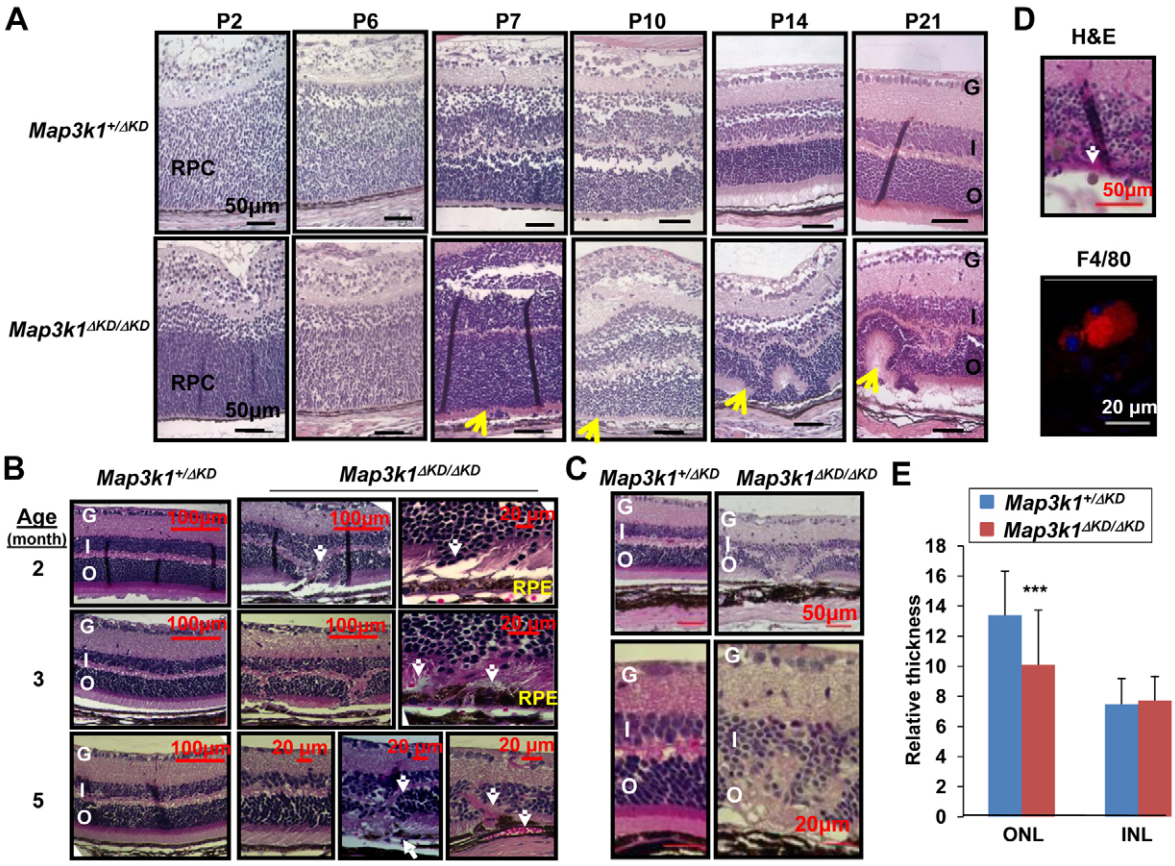

Fig. 2. MAP3K1 is required for postnatal retina development. (**A-D**) The retinas of *Map3k1*$^{+/\Delta KD}$ and *Map3k1*$^{\Delta KD/\Delta KD}$ mice at (A) P2-P21, (B) 2-5 months and (C,D) 1 year, were examined by Hematoxylin and Eosin staining and immunostaining, and were photographed under a microscope. RPC, retinal progenitor cells; G, ganglion cell layer; I, inner nuclear layer; O, outer nuclear layer; RPE, retinal pigment epithelium. Arrows indicate retinal lesions in the *Map3k1*$^{\Delta KD/\Delta KD}$ mice, including (A) malformed retina and rosette formation; and (B) photoreceptor dislocation, RPE breaks and blood vessel invasion. Different pictures of the *Map3k1*$^{\Delta KD/\Delta KD}$ retina are shown to illustrate various pathological features observed. The 1-year-old *Map3k1*$^{\Delta KD/\Delta KD}$ retinas have (C) clear thinner outer nuclear layer and retinal degeneration, and (D) F4/80-positive mononuclear macrophages (arrow, top panel, red, bottom panel). Cell nuclei are labeled with DAPI (blue). Scale bars: 50 μm (if not otherwise specified). (**E**) The thicknesses of the ONL and INL were measured in the 1-year-old *Map3k1*$^{+/\Delta KD}$ and *Map3k1*$^{\Delta KD/\Delta KD}$ mice. Statistical analyses were carried out by comparing the average thickness between the genotypes. Data are mean+s.e.m. ***P<0.001.

At P7, the retinas of the *Map3k1*$^{\Delta KD/\Delta KD}$ mice started to show misallocated cell bodies at the posterior side, whereas at P15 and older, they developed sporadic rosette structures posterior to the photoreceptor layers. By contrast, all the retinas in age-matched *Map3k1*$^{+/\Delta KD}$ mice (n=4) were morphologically normal, with no retinal infolding or rosette formation.

When grown older, the retinas of *Map3k1*$^{+/\Delta KD}$ and *Map3k1*$^{\Delta KD/\Delta KD}$ mice were both fully developed and laminated, but those of the knockout mice displayed a number of pathological changes at 2-12 months of age. These include regional dislocation in the outer nuclear layer (ONL), focal RPE leak, and localized neo-vascularization in RPE and ONL (Fig. 2B). Compared with the 1-year-old *Map3k1*$^{+/\Delta KD}$ retinas, the *Map3k1*$^{\Delta KD/\Delta KD}$ retina had overall thinner ONL and invasion of macrophages (Fig. 2C,D,E), all clear signs of retinal degeneration. Results from this work establish that a single *Map3k1* allele in the heterozygote is sufficient to maintain normal retinal development; however, total MAP3K1 loss in the *Map3k1*$^{\Delta KD/\Delta KD}$ (*Map3k1* knockout) mice results in retinal dysplasia and an early onset of retinal degeneration.

A closed eyelid is required for neonatal development of ocular surface, but not for retinal formation

The *Map3k1*-knockout fetuses survived embryonic development, yet they had an EOB phenotype because of defective embryonic eyelid closure (Zhang et al., 2003). It is possible that the retinal damage in the knockout mice is secondary to EOB, because exposure of dark adapted rats to excessive amounts of light has been shown to cause photoreceptor cell death and retinal degeneration (Hafezi et al., 1997; Reme et al., 2000). To examine this possibility, we performed reciprocal surgical procedures either to suture the opened eyelids of the knockout or to open the closed eyelid of wild-type mice right after birth (P0) (Fig. 3A). The suture was removed at P14, a time point when the eyelid fusion dissolves and lid opens naturally in wild-type mice. Examination of the retinas at P15 showed that the *Map3k1*$^{\Delta KD/\Delta KD}$ mice had a rosette structure in the ONL, regardless of whether their eyelids were surgically sutured; however, the wild-type mice had normal retina with no detectable misfolding and dysplasia, regardless of whether their eyelids were surgically opened at birth (Fig. 3B).

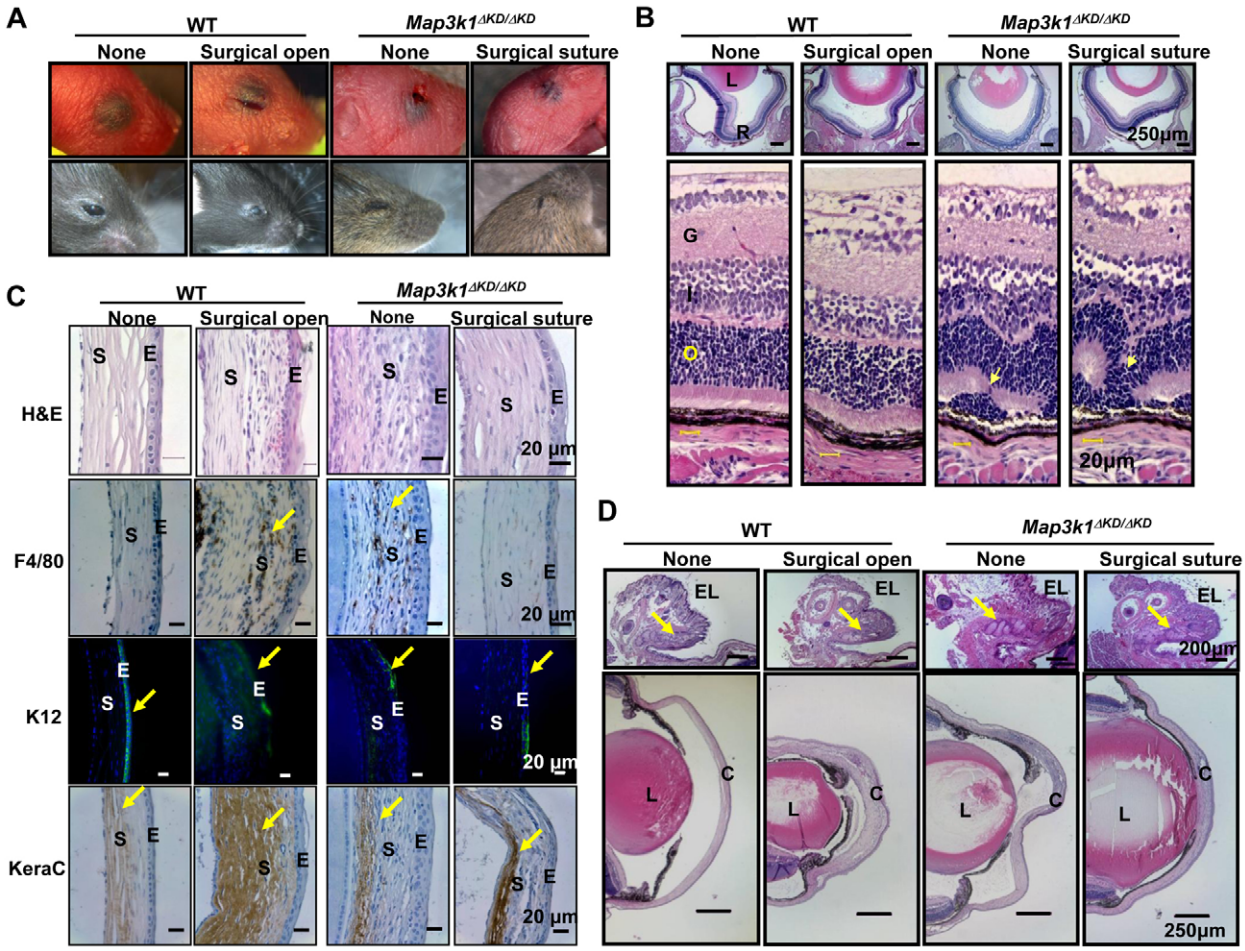

Fig. 3. The role of a closed eyelid in postnatal eye development. Mice were subjected to surgical procedures to open the closed eyelid in wild type and suture the open eyelid in *Map3k1*$^{\Delta KD/\Delta KD}$ mice at P1 and suture was removed at P14. (**A**) Photographs of the eyes without or with the surgical procedures at P1 (top panels) and P15 (bottom panels). (**B**) The eyes at P15 were subjected to Hematoxylin and Eosin staining, and the retinas were examined under the microscope. L, lens; R, retina; G, ganglion layer; I, inner nuclear layer; O, outer nuclear layer. Clear retinal folding (arrows) is found in the *Map3k1*$^{\Delta KD/\Delta KD}$ mice regardless of whether the eyelid is sutured. (**C**) The corneas of the mice were subjected to Hematoxylin and Eosin staining, and immunohistochemistry with chromogenic reporters for macrophages (F4/80) and stromal keratocyte marker (keratocan), and with fluorescent reporter for corneal epithelial specific keratin 12 (K12, green) and DAPI for nuclei (blue). Surgical eyelid open in the wild-type mice causes severe corneal pathology (arrows), including macrophage invasion, loss of K12 expression and increased keratocan, similar to the knockout mice. S, corneal stroma; E, corneal epithelium. (**D**) The anterior surface of the eye was examined after Hematoxylin and Eosin staining. EL, eyelid; L, lens; C, cornea. MAP3K1 loss and eyelid suture do not affect Meibomian gland (arrows) formation in the eyelid (upper panels), but an opened eyelid at birth is clearly associated with corneal abnormalities (lower panels).

In addition to retina abnormalities, the knockout mice grew up with clear pathologies at the anterior surface of the eye, including cloudiness of the cornea, stromal neovascularization and thickening, and iris overgrowth, whereas they appeared to have normal Meibomian glands (Fig. 3C,D). Immunohistochemistry analyses showed that the *Map3k1*-knockout corneas lost expression of keratin 12 (K12), a specific marker for corneal epithelium, and had macrophage invasion, as detected by the expression of F4/80, in the stroma, which is indicative of abnormal and dysfunctional cornea. Interestingly, surgical suture of the eyelid in knockout mice partially restored normal corneal appearance, and reduced corneal thickening and macrophage invasion (Fig. 3C,D). Conversely, surgical eyelid opening in wild-type mice resulted in significant macrophage invasion and lost K12 expression, mimicking abnormalities observed in the knockout mice. Based on these observations, we suggest that a closed eyelid at birth is required for ocular surface development and maturation during early postnatal stages, but is not essential for postnatal retina development. The retinal damage in the MAP3K1-knockout mice is therefore not secondary to EOB.

The retinal defect in the *Map3k1*$^{\Delta KD/\Delta KD}$ mice was not due to insufficient JNK activity

Previously, we have shown that the *Map3k1* heterozygous mice had normal eyelid development, but *Map3k1* became haploinsufficient for eyelid closure in the *Jnk1*$^{-/-}$ and *Jnk1*$^{+/-}$*Jnk2*$^{+/-}$ mice (Takatori et al., 2008). This is because the *Map3k1/Jnk* compound mutant mice have insufficient JNK signaling needed for eyelid closure. To determine whether the MAP3K1-JNK axis was involved also in retinal development, we examined the retinas of compound mutant mice. The *Map3k1*$^{+/\Delta KD}$*Jnk1*$^{-/-}$ and *Map3k1*$^{+/\Delta KD}$*Jnk1*$^{+/-}$*Jnk2*$^{+/-}$ mice (n=4) clearly had EOB at P1, but the *Map3k1*$^{+/\Delta KD}$*Jnk1*$^{+/-}$

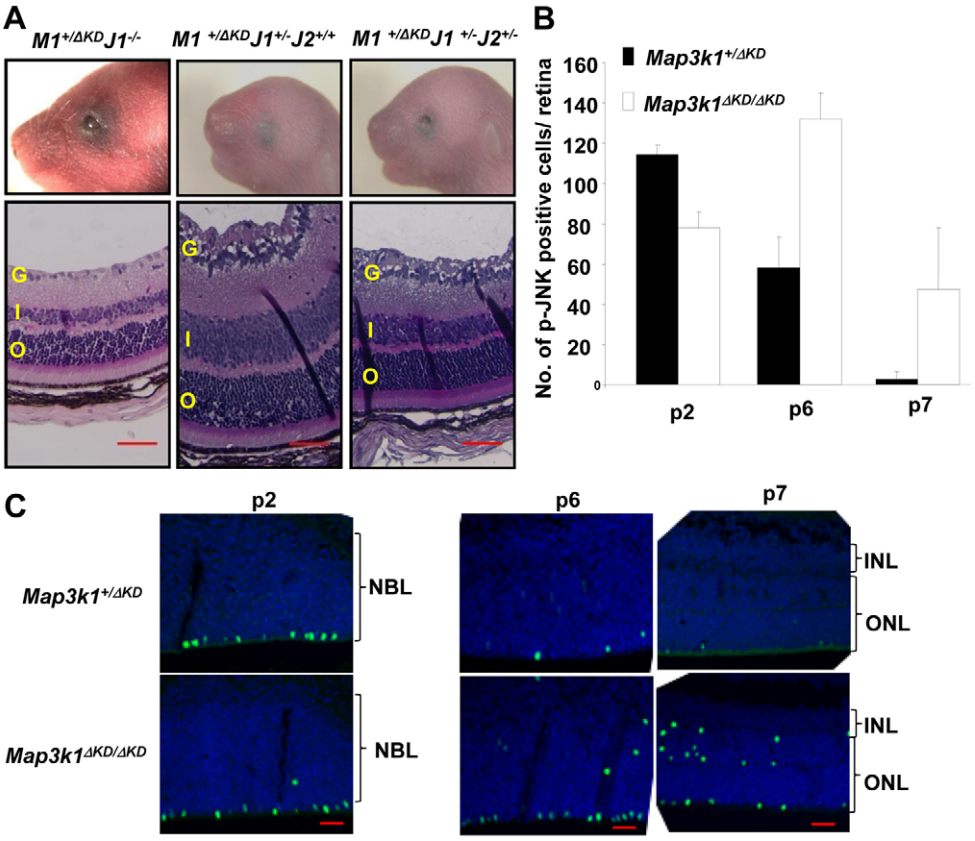

Fig. 4. Retinal defects of the *Map3k1*$^{\Delta KD/\Delta KD}$ mice are independent of EOB and JNK. (**A**) Compound transgenic mice were photographed at P1 (top panels) and their retinas were examined at P15 by Hematoxylin and Eosin staining (bottom panels). The *Map3k1*$^{+/\Delta KD}$*Jnk1*$^{-/-}$ and *Map3k1*$^{+/\Delta KD}$*Jnk1*$^{+/-}$*Jnk2*$^{+/-}$ mice show clear EOB, whereas the *Map3k1*$^{+/\Delta KD}$*Jnk1*$^{+/-}$ mice have closed eyelids at birth. All the compound mice have normal retina development. (**B**,**C**) The retinas of *Map3k1*$^{+/\Delta KD}$ and *Map3k1*$^{\Delta KD/\Delta KD}$ mice at different postnatal ages were examined by immunostaining for p-JNK. Pictures were taken under fluorescent microscopy (C) and p-JNK-positive cells were quantified (B). Results represent four sections/eye and four eyes for each genotype and developmental stage. Data are mean+s.e.m. G, ganglion layer; INL, inner nuclear layer; ONL, outer nuclear layer; NBL, neuroblastic layer. Scale bars: 50 μm.

mice had a closed eyelid, similar to what has been reported previously (Takatori et al., 2008) (Fig. 4A). Nevertheless, all mice exhibited normal retinal morphology, regardless whether they had EOB, indicating again that retinal abnormality is not secondary to defective eyelid closure.

The above observations also imply that MAP3K1 regulates retinal development through a JNK-independent mechanism. To further evaluate this idea, we examined retinas for the presence of phospho-JNK, which is the enzymatically active form of this kinase. Phospho-JNK-positive cells were detected at the outer edge of the P2 retina, and the number of positive cells was similar in *Map3k1*$^{+/\Delta KD}$ and *Map3k1*$^{\Delta KD/\Delta KD}$ mice (Fig. 4B,C). Although the number of p-JNK-positive cells was decreased at P6 and was almost undetectable at P7 in the heterozygous retinas, it was still quite abundant at P6 and P7 in the knockout retinas. In addition, some p-JNK-positive cells were found in ectopic positions in the inner layer of the knockout retinas. These results suggest that aberrant retinal development in the knockout mice is not due to insufficient amounts of active JNK.

Perturbed proliferation and apoptosis of the *Map3k1*-knockout retina

At late embryonic and neonatal stages, the RPCs either proliferate to populate the growing retina or exit the cell cycle to differentiate into functionally specialized cells. To examine whether MAP3K1 loss affects cell proliferation, we examined retinas for phosphohistone H3, an M phase marker that labels mitotic progenitors. The M-phase progenitors are known to be distinctly located at the sclera side of the RPC layers. Accordingly, we detected the p-H3-positive cells confined to the outer edge of the RPC layers, whereas the number of p-H3-positive cells was most abundant at P2, markedly reduced at P6, and almost diminished at P7 and P8 in the retinas of the heterozygous mice (Fig. 5A,B). Compared with that in heterozygote, the number of p-H3-positive cells in knockout mice was similar at P2, slight increased at P6, and significantly higher at P7 and P8 (Fig. 5A,B; data not shown). In addition to more mitotic cells at the outer edge, the knockout mice had some p-H3-positive cells located in unusual positions in the inner segment of the retinas (Fig. 5B). Mitosis ceased at P12 in the retinas of both genotypes.

After mitosis, the somas of the progenitors migrate to the vitreal side of the RPC layers where they complete S phase. The detection of more abundant mitotic cells in the outer segment of the knockout retinas suggests that MAP3K1 loss may promote the progenitor cells to cycle faster and for an extended period of time. In this case, the number of S-phase cells would also be higher in the knockout retina. To examine this possibility, we measured the expression of proliferating cell nuclear antigen (PCNA), an S-phase marker. Similar to the mitotic cells, the S-phase-positive cells were more abundant at P2, but gradually reduced in number when the mice grew older and became undetectable at P12 in both genotypes (Fig. 5C; data not shown). Although the fraction of PCNA-positive cells in *Map3k1*$^{+/\Delta KD}$ and *Map3k1*$^{\Delta KD/\Delta KD}$ retinas was slightly, but insignificantly, different at P2, it was significantly different at P6-P10 (Fig. 5C; Table 1). Specifically, the retinas of knockout mice displayed more abundant PCNA staining than did their age-matched heterozygote counterparts, especially in peripheral regions of the retina.

The RPCs are oriented radially along the apical/basal axis with their end feet anchored at both sides. To determine whether the mislocated mitotic cells in the *Map3k1*$^{\Delta KD/\Delta KD}$ retinas were due to loss of cell polarity and adhesion, we examined F-actin levels,

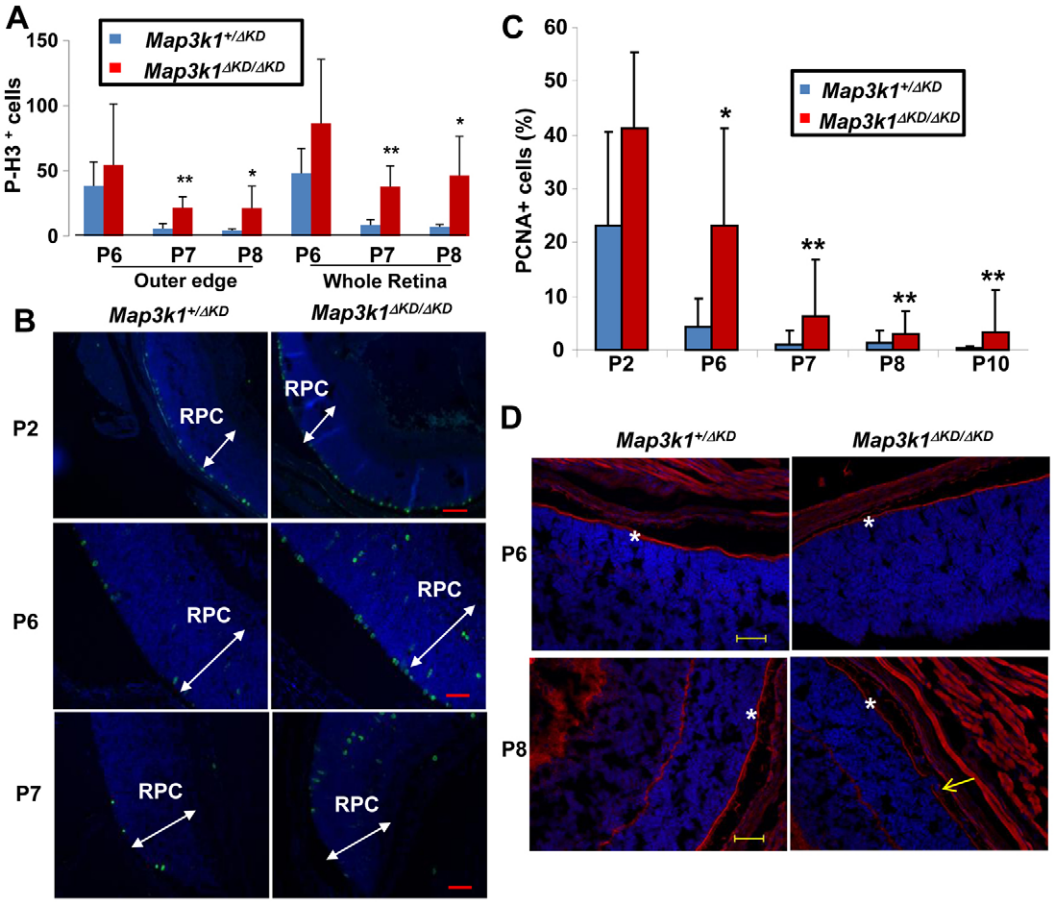

Fig. 5. Aberrant proliferation in the retinas of *Map3k1*$^{\Delta KD/\Delta KD}$ mice. (**A-C**) Eyes isolated from *Map3k1*$^{+/\Delta KD}$ and *Map3k1*$^{\Delta KD/\Delta KD}$ mice at different postnatal ages were subjected to immunostaining with anti-p-H3 to detect mitotic cells and anti-PCNA to detect cells in S phase. Mitotic cells (green) and total cells (blue) were photographed under fluorescent microscopy (B). The retina progenitor cell (RPC) layers are indicated by arrows. p-H3-positive (A) and PCNA-positive (C) cells were quantified in the whole and outer segments of the retinas. Statistical analyses were carried out by comparing the numbers in different genotypes. Data are mean+s.e.m. *P<0.05, **P<0.01. (**D**) Retinas were labeled with fluorescent-labeled phalloidin. Pictures were taken under fluorescent microscopy. The outer segment is labeled by asterisks and the retinal folding is indicated by an arrow. Scale bars: 100 μm for P2; 50 μm for P6-P8.

which is abundant at the cell feet attaching to apical surfaces. F-actin was clearly seen at the apical surfaces of the p6 and p8 retinas, and importantly, its expression pattern was identical in *Map3k1*$^{+/\Delta KD}$ and *Map3k1*$^{\Delta KD/\Delta KD}$ retinas (Fig. 5D). The F-actin in the *Map3k1*$^{\Delta KD/\Delta KD}$ retinas was interrupted only in the regions where the retinal folding occurred, but it was otherwise largely intact at the apical surface and was not detected in ectopic areas. MAP3K1 loss therefore does not seem to perturb cell polarity and adhesion.

The developing retina tends to establish the correct balance between proliferation and size; therefore, excessive cellular proliferation often triggers cell death. To determine whether this were the case, we performed a TUNEL assay to examine retinas of heterozygous and knockout mice. At ages younger than P10, there was no major difference in apoptosis between *Map3k1*$^{+/\Delta KD}$ and *Map3k1*$^{\Delta KD/\Delta KD}$ retinas. At ages P14-P21, the number of apoptotic cells was significantly higher in the retinas of knockout than in heterozygous mice (Fig. 6A,B; Table 2). Apoptotic cells were detected in a random pattern in both inner and outer nuclear layers, suggesting that death was not selective to a specific cell type (Table 2).

MAP3K1 affects retinal cell differentiation

To determine whether the increased proliferation and apoptosis in the *Map3k1* mutant retina resulted in aberrant production of specific cell types, we examined several classes of retinal cells in P21 *Map3k1*$^{+/\Delta KD}$ and *Map3k1*$^{\Delta KD/\Delta KD}$ mice (n=4). In contrast to the early-born horizontal (calbindin positive) and amacrine (calbindin positive) cells, and the late-born bipolar cells (PKCα positive) and rods (rhodopsin positive), which were not different between the *Map3k1*$^{+/\Delta KD}$ and *Map3k1*$^{\Delta KD/\Delta KD}$ retinas, the late-born Müller glial cells (glutamine synthetase positive) were significantly more abundant in the *Map3k1*-knockout retinas (Fig. 7A). The Müller glial cells offer a physical scaffold for retinal organization; thus, their overproduction may perturb retinal architecture in the *Map3k1*-knockout mice. To test this possibility,

Table 1. PCNA-positive cells in the developing retina

	Peripheral			Middle			Central		
Stage	Wild type	Knockout	*P*-value	Wild type	Knockout	*P*-value	Wild type	Knockout	*P*-value
P2	25.66±25	48.47±2.5	0.11	19±10	45.53±10.7	0.63	24.94±15.18	29.74±18.24	0.63
P6	11.69±13	23.83±19	0.06	8±7.2	33.65 ±23.4	0.01	4.44±2.22	11.7±8.55	0.01
P7	2.44±4.5	14.58±4.13	0.002	0.056±0.14	3.479±6.26	0.06	0±0	0.58±1.12	0.08
P8	3.28±3	7.48±4.1	0.003	0.316±0.46	1.736±0.73	1.6×10^{-6}	0.00037±0.0009	0.0049±0.004	4.9×10^{-5}
P10	1.2±0.3	8.59±12	0.006	0.036±0.09	1.339±1.69	0.006	0.135±0.21	0.202±0.311	0.544

Shown is the percentage (±s.d.) of PCNA-positive cells in each area of the developing retina.

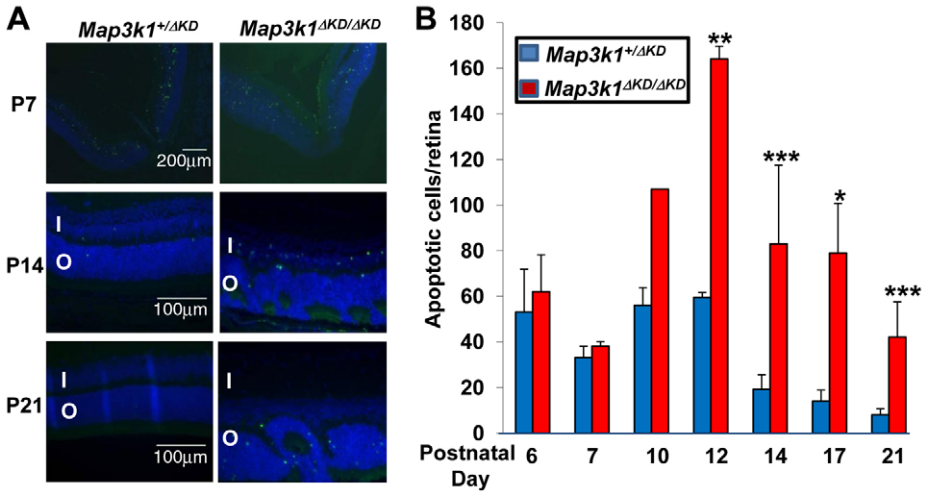

Fig. 6. Increased apoptosis in the retinas of *Map3k1*$^{\Delta KD/\Delta KD}$ mice. The eyes isolated from *Map3k1*$^{+/\Delta KD}$ and *Map3k1*$^{\Delta KD/\Delta KD}$ mice at different postnatal ages were subjected to TUNEL assays. (**A**) Pictures were taken under fluorescent microscopy. I, inner nuclear layer; O, outer nuclear layer. (**B**) The average number of apoptotic cells per retina was quantified+s.e.m.. Results represent at least four eyes at each developmental stage and genotype. Statistical analyses were carried out by comparing the numbers in different genotypes. **P*<0.05, ***P*<0.01, ****P*<0.001.

we examined the P21 and P90 retinas, focusing on the hyperplasic lesions in knockout mice and the corresponding areas in heterozygote. Although the Müller glial processes (glutamine synthetase positive) were confined between the inner and outer limiting membrane in the heterozygous retinas, they protruded beyond the boundary of the outer limiting membrane and displaced the rod photoreceptors in hyperplasic lesions in the knockout retinas (Fig. 7B). Misallocated bipolar (PKCα positive) and horizontal (calbindin positive) cells were detected occasionally in some lesions, but the rod (rhodopsin positive) and cone (opsin positive) photoreceptors were affected in all the dysplastic lesions in the knockout mice.

To assess at which developmental stage Müller glia was deregulated in the knockout retinas, we examined retinas at different postnatal ages. The glutamine synthetase-positive cells were first detected at P7 and became more abundant at P10 and P21. Although these cells were confined to a thin layer in the INL in the *Map3k1*$^{+/\Delta KD}$ retinas, they were more abundant and displayed a diffused pattern in the *Map3k1*$^{\Delta KD/\Delta KD}$ retinas (Fig. 7C). A closer examination of the knockout retinas showed that the soma of some glutamine synthetase-positive cells were misallocated outside of INL and scattered towards the ONL (Fig. 8A). Interestingly, the misallocated glutamine synthetase-, p-JNK- and p-H3-positive cells displayed similar distribution patterns, raising the possibility that they were all mitotic cells in nature. As antibodies for co-immunostaining were not available to test this idea, we examined the nuclear morphology and found that all these cells had condensed nuclei (Fig. 8B). These results suggest that MAP3K1 loss may lead to re-activation of Müller glia proliferation and gliosis.

Activation of the RB/E2F pathways in MAP3K1-null retina

The aberrant proliferation and apoptosis, and Müller glia overproduction in the *Map3k1*-knockout retinas were similar to those occurring in the *Rb*- and *p27*^{kip1}-knockout retinas. We therefore asked whether MAP3K1 affected the cell cycle regulatory pathways. Although the expression of RB and p27^{kip1} was not affected by MAP3K1 loss, the expression of cyclin D1 (*Ccnd1*) and CDK4/6 (*Cdk4/6*), which are downstream effectors of p27^{kip1}, was three- to sixfold higher in the knockout retinas (Fig. 8C). The Cyclin/CDKs are known to phosphorylate RB, thereby removing the inhibitory effects of RB on E2F, resulting in activation of E2F and its target gene expression. By examining the lysates of developing retinas, we found that phospho-RB was indeed detected in the knockout but not heterozygous mice (Fig. 8D). By examining RNA of developing retinas, we found that, although expression of *E2f1* itself was unaffected by MAP3K1 loss, expression of several known E2F-target genes, such as dihydrofolate reductase (*Dhfr*), polymerase alpha 1 (*Pola1*), cyclin A (*Ccna*) and cyclin E (*Ccne*), were upregulated two- to fivefold in the knockout mice (Fig. 8E). These results were consistent with previous findings that *Map3k1*$^{\Delta KD/\Delta KD}$ retinas had more PCNA, a target gene of the E2F complexes. Taken together, these results

Table 2. TUNEL-positive cells in developing retina

	Heterozygote			Knockout			*P*-value		
Stage	INL	ONL	Total	INL	ONL	Total	INL	ONL	Total
P6			53±18.85			62.25±16.19			0.44
P7			33±4.97			38.5±2.12			0.22
P10			56.5±7.78			107			NA
P12			59.5±2.12			164±5.66			0.0017
P14	7.45±3.58	11.9±4.24	19.24±6.29	60.95±26.53	21.95±9.74	83±34.61	8.9×10^{-11}	0.0001	4.3×10^{-10}
P14 open EL	7.47±3.02	12±5.7	19.5±6.55						
P17	0.5±0.7	13±4.24	13±4.95	43.75±14.2	36.75±10.1	79±21.8	0.015	0.048	0.012
P21	0.75±0.75	7±2.63	8±2.67	2.73±2.37	40±15.05	42±15.51	0.012	2.1×10^{-7}	1.38×10^{-7}

Shown is the number (±s.d.) of TUNEL-positive cells in the inner (INL) and outer (ONL) nuclear layers of the developing retina. For P6 to P12, INL and ONL cannot be distinguished and a total value is given. EL, eyelid; NA, not applicable.

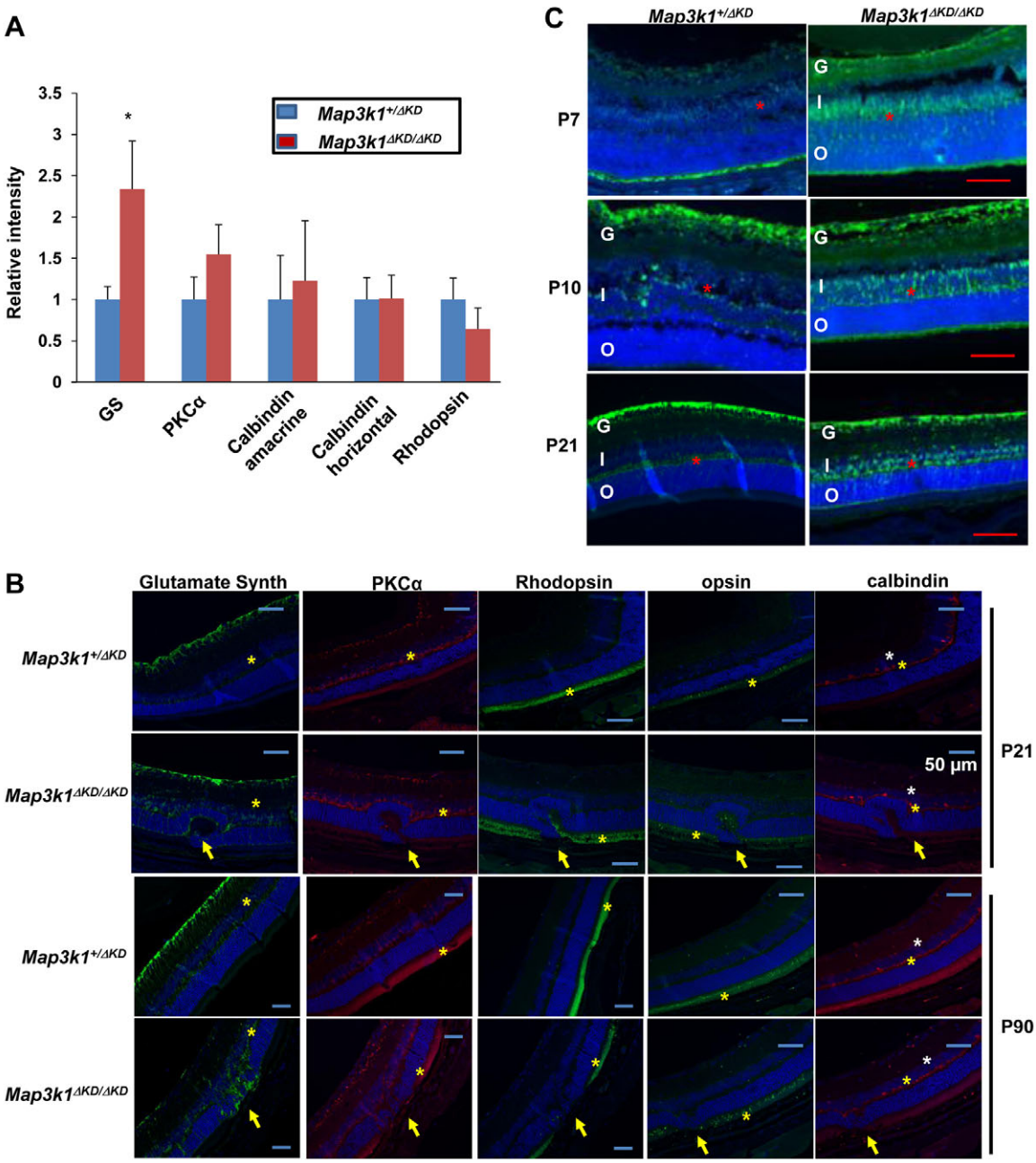

Fig. 7. MAP3K1 inhibits Müller glial cell proliferation. (A,B) Eyes isolated from *Map3k1*$^{+/\Delta KD}$ and *Map3k1*$^{\Delta KD/\Delta KD}$ mice were subjected to immunostaining using various antibodies as indicated. (**A**) Staining intensity was measured in P21 eyes. Results represent the average of at least four retinas of each genotype and statistical analyses were carried out by comparing the numbers in different genotypes. Data are mean+s.e.m. *P<0.05. (**B**) Pictures of anti-glutamine synthetase (green; Müller cells), anti-PKCα (red; bipolar cells), anti-calbindin [red; horizontal cells (yellow asterisks) and amacrine (white asterisks)], anti-rhodopsin (green; rods) and anti-opsin (green; cone) staining taken under fluorescent microscopy. Nuclei were stained by DAPI (blue). Positive stained cell layers are marked by asterisks and abnormal retina folding in the knockout mice is indicated with arrows. Scale bars: 50 μm. (**C**) Photographs of immunostaining by anti-glutamine synthetase of retinas at different postnatal ages. Positive stained cell layers are marked by red asterisks. G, ganglion layer; I, inner nuclear layer; O, outer nuclear layer. Scale bars: 100 μm.

suggest that MAP3K1 loss is associated with an increase of CDK/cyclin D1 and p-RB, which may in turn lead to activation of E2F1 and its target gene expression in the developing retina.

DISCUSSION

Recent studies of the MAP3K1-deficient mice have uncovered numerous cell type- and tissue-specific roles of MAP3K1 in development, homeostatic maintenance and disease processes (Xia and Karin, 2004). Here, we show that MAP3K1 is highly expressed in the developing retinas, where it regulates cell proliferation and apoptosis. Cyclin D1 is known to regulate RPC proliferation by promoting G1- to S-phase transition in dividing cells through activation of cyclin-dependent kinases 4 and 6 (CDK4/6), while the CDKs in turn lead to phosphorylation and inactivation of RB, thereby enhancing E2F activity for gene expression and DNA replication (Das et al., 2009). We suggest that MAP3K1 suppresses

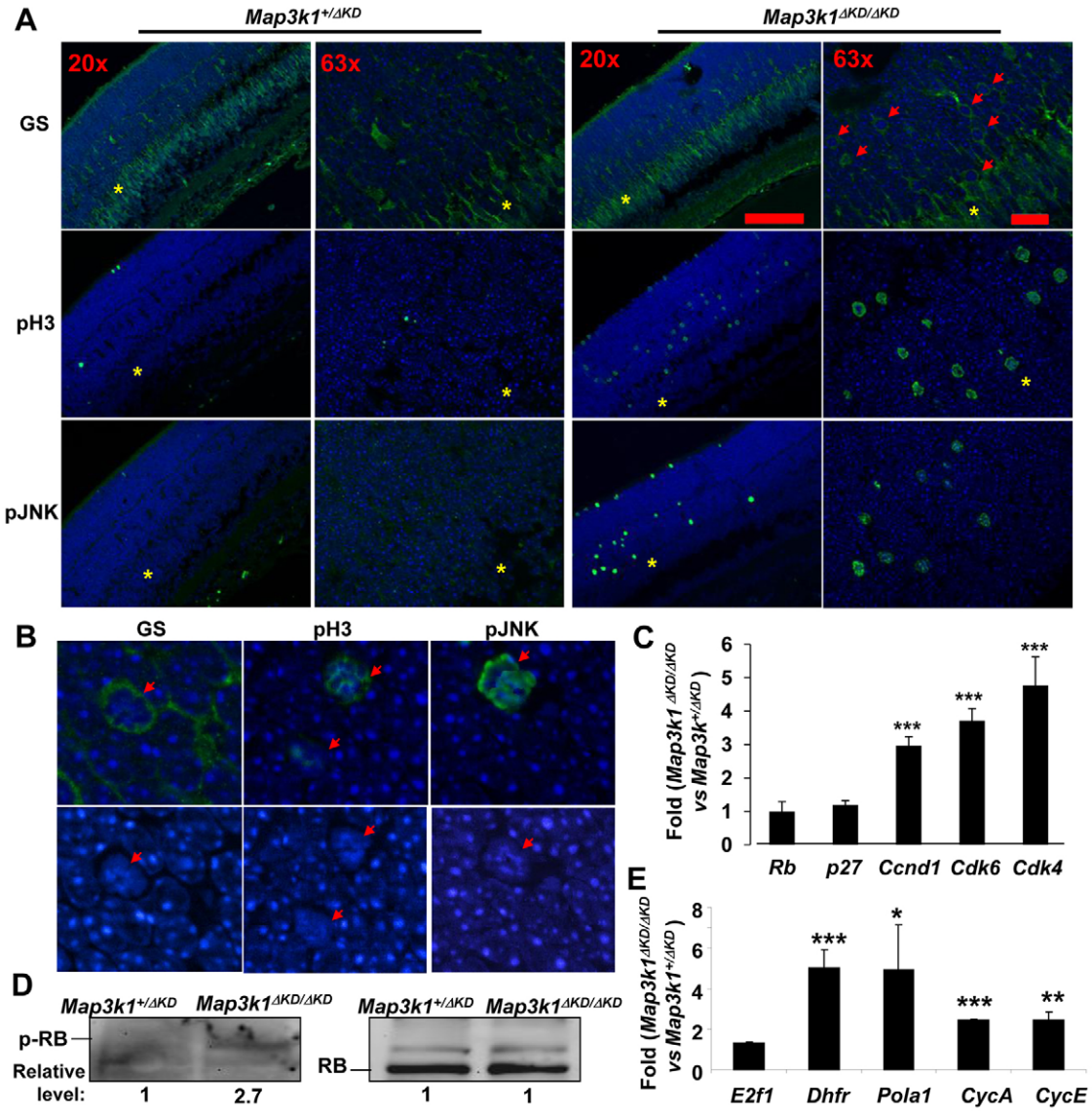

Fig. 8. Activation of the E2F1 pathways in the retinas of *Map3k1*$^{\Delta KD/\Delta KD}$ mice. (**A**,**B**) Immunostaining of the P7 *Map3k1*$^{+/\Delta KD}$ and *Map3k1*$^{\Delta KD/\Delta KD}$ retinas with various antibodies and pictures were taken under various magnifications, as indicated. The inner nuclear layer is labeled with asterisks and cells with condensed nuclei are labeled with arrows. (**C**,**E**) RNA isolated from the retinas of *Map3k1*$^{+/\Delta KD}$ and *Map3k1*$^{\Delta KD/\Delta KD}$ mice at P7 were subjected to real-time RT-PCR to examine the expression of (C) genes that may affect RB, including *Rb1*, *p27*^{kip1}, *Ccnd1*, *Cdk4* and *Cdk6*, and (E) *E2f1* and its target genes, *Dhfr*, *Pola1*, *Ccna* and *Ccne*. The levels of expression in the retinas of *Map3k1*$^{\Delta KD/\Delta KD}$ mice were compared with those in *Map3k1*$^{+/\Delta KD}$ mice, which were set as 1. Results are average of at least four samples of each genotype. Data are mean+s.e.m. **P*<0.05, ***P*<0.01, ****P*<0.001. (**D**) Lysates of the P7 retinas were analyzed by western blotting for p-RB and total-RB, as indicated. The relative expression in the *Map3k1*$^{\Delta KD/\Delta KD}$ was compared with that in *Map3k1*$^{+/\Delta KD}$, which was set as 1.

this pathway, as MAP3K1 ablation leads to increased expression of cyclin D1, CDK4 and CDK6, RB phosphorylation, and E2F activation in the neonatal retinas. Consistent with this idea, the *Map3k1*-knockout mice share great phenotypic similarities with the *E2f1*-transgenic and *Rb*-knockout mice, all displaying increased proliferation followed by apoptosis and formation of rosette-like structures in the developing retinas (Lin et al., 2001). Consequently, the *Map3k1*-knockout retinas have photoreceptor loss, blood vessel invasion, RPE break down and early onset of retinal degeneration.

Despite of their phenotypic similarities, the *Map3k1*- and *Rb*-knockout mice have different developmental defects in the retina. First, both *Map3k1*- and *Rb*-knockout retinas display higher mitotic index, with the mitotic cells located along the outer edge of the RPC layers and ectopically at unusual positions in the inner layers (Chen et al., 2004). Nonetheless, the *Map3k1*-knockout retinas have a higher level of mitotic cells at the outer edge and the *Rb* knockouts do not. Second, RB is involved in cell cycle exit of differentiated precursors, and consequently, the *Rb* knockout has an imbalanced production of precursors and misrepresentation of multiple retinal cell types (Chen et al., 2007; Lin et al., 2001). Unlike RB, however, MAP3K1 loss causes overproduction of Müller glia cells with no apparent impact on other cell populations. Third, in the *Map3k1*-knockout retina, some Müller glia nuclei seem to undergo mitosis and migrate out of INL, indicating

proliferative gliosis. It is, thus, possible that reactivated Müller glial cells migrate to the outer edge, where they behave like progenitor cells and contribute to the hyper-mitotic phenotype in this region. The proliferative gliosis does not occur in the *Rb*-knockout mice, but, interestingly, it is observed in mice lacking $p27^{kip1}$, an upstream inhibitor of CDK (Dyer and Cepko, 2000; Levine et al., 2000). In addition to our findings in retinal progenitor cells, MAP3K1 is shown to be involved in CD40 ligand-induced cyclin D2 expression and proliferation in B cells (Gallagher et al., 2007). Thus, MAP3K1 may act as a negative regulator of the CDK-RB-E2F pathway in multiple cell types.

As MAP3K1 is not required for $p27^{kip1}$ expression, we suggest that MAP3K1 must act in parallel to $p27^{kip1}$ in regulating gliosis. Besides the RB-E2F pathways, MAP3K1 may crosstalk with other regulatory networks during retinal development. One candidate is the Notch-Hes pathway. Notch signaling determines the commitment of late RPCs to either neuronal or glial cell fate, thus the increase in Müller glia is at the expense of other late-born cells (Furukawa et al., 2000). This is not the case for the *Map3k1*-knockout retinas, in which the increased Müller glia is not associated with decreased rods and bipolar cells. On the other hand, MAP3K1 may regulate cell polarity, important for interkinetic nuclear migration. The polarity defects can perturb cell migration, leading to dissociation of the mitotic cells from the outer edge of RPC layer and dislocation to the INL (Sottocornola et al., 2010). The mitotic index at the outer edge was increased, not decreased, whereas the F-actin at the apical surface marking adhesion junction was largely intact in the knockout retinas. It is therefore unlikely that MAP3K1 loss perturbs cell polarity and hence mitotic cell migration. Although the identity of the molecular factors that link MAP3K1 and the RB-E2F pathway has remained a mystery, further investigation into this issue may help to better understand the underlying mechanism of reactive gliosis, which is associated with major diseases of the retina, including retinitis pigmentosa (Fariss et al., 2000; Li et al., 1995), macular degeneration (Kimura et al., 1999) and diabetic retinopathy (Amin et al., 1997).

Müller glial cell reactivation usually takes place in response to acute retinal stress or injury (Jadhav et al., 2009), it is therefore important to confirm that retina defects in the *Map3k1*-knockout mice are not due to external stress associated with EOB. The MAP3K1 is well characterized for its role in eyelid morphogenesis (Zhang et al., 2003). During eyelid development, MAP3K1 is required for JNK activation, which in turn leads to eyelid tip epithelial cell migration and embryonic eyelid closure (Takatori et al., 2008). In addition to eyelid development, MAP3K1 also acts through JNK to regulate diverse physiological and pathological processes. We show for the first time that MAP3K1 has a JNK-independent function in retina development. Two pieces of evidence support this conclusion. First, the developing retina of the knockout mice has higher JNK activation associated with mitosis, suggesting that the M phase JNK phosphorylation is independent of MAP3K1 (Ho and Li, 2010). Second, only the $Map3k1^{\Delta KD/\Delta KD}$ mice display abnormal retinal development, whereas the compound mutant $Map3k1^{+/\Delta KD}Jnk1^{-/-}$ and $Map3k1^{+/\Delta KD}Jnk1^{+/-}Jnk2^{+/-}$ mice have reduced JNK yet normal retina development. Hence, the retinal defects in the knockout mice are not associated with inactivation of JNK.

The EOB phenotype in the MAP3K1-knockout mice raises the possibility that light transmission through the 'open eyelid' is responsible for damage of the developing retina. However, our experimental evidence has ruled out this possibility. We show that suturing the 'opened eyelids' at birth of the knockout mice does not rescue the retinal defects, whereas surgically open 'closed eyelids' at birth of wild-type mice does not cause retina abnormalities. Additionally, the $Map3k1^{+/\Delta KD}Jnk1^{-/-}$ and $Map3k1^{+/\Delta KD}Jnk1^{+/-}Jnk2^{+/-}$ mice have EOB, but they do not develop retinal lesions in the same way as the $Map3k1^{\Delta KD/\Delta KD}$ mice. Furthermore, studies in lamb show that strong light sources used with fetal endoscopy do not cause morphological retinal damage in fetal eyes (Deprest et al., 1999). Defective retina development in the knockout mice therefore is unlikely to be secondary to defective eyelid closure.

Modulation of signaling pathway activity with great precision can ensure robustness and reproducibility of cell fate specification. In *Drosophila*, the Ras, PAK, Raf, TAK and MAPK are all implicated in photoreceptor differentiation (Dickson et al., 1995; Halfar et al., 2001; Menzel et al., 2007; Mihaly et al., 2001); however, a *Drosophila* MAP3K1 is yet to be identified. In mammals, many signaling factors are found activated in temporal correlation with crucial events of retina maturation, but their roles in retinal cell fate determination remain poorly understood (Oliveira et al., 2008). So far, the mammalian ASK1-p38 pathway is linked to post-mitotic cell apoptosis (Campos et al., 2006; Harada et al., 2006), whereas the PI3K-AKT pathway mediates cell survival (O'Driscoll et al., 2006). Results from this work uncover a new signaling mechanism through which MAP3K1 may act through the RB-E2F axis in prevention of retinal malformation and degeneration. Further investigating the roles MAP3K1 play in Müller glial cell re-activation may lead to therapeutic strategies for retinal repair and injury protection.

Acknowledgements

We thank Drs Shuzhen Wang (UAB) for analyzing the fetal retinas, Donald Fox (University of Houston, TX, USA) for discussing the data and suggestions, and Alvaro Puga (University of Cincinnati, OH, USA) for critical reading of the manuscript. This research was supported by NIH grant EY15227 (to Y.X.), by Research to Prevent Blindness and by Ohio Lions Eye Research Foundation. Deposited in PMC for release after 12 months.

Competing interests statement

The authors declare no competing financial interests.

References

Ajioka, I. and Dyer, M. A. (2008). A new model of tumor susceptibility following tumor suppressor gene inactivation. *Cell Cycle* **7**, 735-740.

Amin, R. H., Frank, R. N., Kennedy, A., Eliott, D., Puklin, J. E. and Abrams, G. W. (1997). Vascular endothelial growth factor is present in glial cells of the retina and optic nerve of human subjects with nonproliferative diabetic retinopathy. *Invest Ophthalmol. Vis. Sci.* **38**, 36-47.

Campos, C. B., Bedard, P. A. and Linden, R. (2006). Requirement of p38 stress-activated MAP kinase for cell death in the developing retina depends on the stage of cell differentiation. *Neurochem. Int.* **49**, 494-499.

Chen, D., Livne-Bar, I., Vanderluit, J. L., Slack, R. S., Agochiya, M. and Bremner, R. (2004). Cell-specific effects of RB or RB/p107 loss on retinal development implicate an intrinsically death-resistant cell-of-origin in retinoblastoma. *Cancer Cell* **5**, 539-551.

Chen, D., Opavsky, R., Pacal, M., Tanimoto, N., Wenzel, P., Seeliger, M. W., Leone, G. and Bremner, R. (2007). Rb-mediated neuronal differentiation through cell-cycle-independent regulation of E2f3a. *PLoS Biol.* **5**, e179.

Chow, R. L. and Lang, R. A. (2001). Early eye development in vertebrates. *Annu. Rev. Cell Dev. Biol.* **17**, 255-296.

Cuevas, B. D., Winter-Vann, A. M., Johnson, N. L. and Johnson, G. L. (2006). MEKK1 controls matrix degradation and tumor cell dissemination during metastasis of polyoma middle-T driven mammary cancer. *Oncogene* **25**, 4998-5010.

Das, G., Choi, Y., Sicinski, P. and Levine, E. M. (2009). Cyclin D1 fine-tunes the neurogenic output of embryonic retinal progenitor cells. *Neural Dev.* **4**, 15.

Deng, M., Chen, W. L., Takatori, A., Peng, Z., Zhang, L., Mongan, M., Parthasarathy, R., Sartor, M., Miller, M., Yang, J. et al. (2006). A role for the mitogen-activated protein kinase kinase kinase 1 in epithelial wound healing. *Mol. Biol. Cell* **17**, 3446-3455.

Deprest, J. A., Luks, F. I., Peers, K. H., D'Olieslager, J. and Van, G. R. (1999). Natural protective mechanisms against endoscopic white-light injury in the fetal lamb eye. *Obstet. Gynecol.* **94**, 124-127.
Dickson, B. J., Dominguez, M., van der, S. A. and Hafen, E. (1995). Control of Drosophila photoreceptor cell fates by phyllopod, a novel nuclear protein acting downstream of the Raf kinase. *Cell* **80**, 453-462.
Downward, J. (1997). Cell cycle: routine role for Ras. *Curr. Biol.* **7**, R258-R260.
Dyer, M. A. and Cepko, C. L. (2000). Control of Muller glial cell proliferation and activation following retinal injury. *Nat. Neurosci.* **3**, 873-880.
Fariss, R. N., Li, Z. Y. and Milam, A. H. (2000). Abnormalities in rod photoreceptors, amacrine cells, and horizontal cells in human retinas with retinitis pigmentosa. *Am. J. Ophthalmol.* **129**, 215-223.
Furukawa, T., Mukherjee, S., Bao, Z. Z., Morrow, E. M. and Cepko, C. L. (2000). rax, Hes1, and notch1 promote the formation of Muller glia by postnatal retinal progenitor cells. *Neuron* **26**, 383-394.
Gallagher, E., Enzler, T., Matsuzawa, A., Anzelon-Mills, A., Otero, D., Holzer, R., Janssen, E., Gao, M. and Karin, M. (2007). Kinase MEKK1 is required for CD40-dependent activation of the kinases Jnk and p38, germinal center formation, B cell proliferation and antibody production. *Nat. Immunol.* **8**, 57-63.
Gao, M., Labuda, T., Xia, Y., Gallagher, E., Fang, D., Liu, Y. C. and Karin, M. (2004). Jun turnover is controlled through JNK-dependent phosphorylation of the E3 ligase Itch. *Science* **306**, 271-275.
Hafezi, F., Marti, A., Munz, K. and Reme, C. E. (1997). Light-induced apoptosis: differential timing in the retina and pigment epithelium. *Exp. Eye Res.* **64**, 963-970.
Halfar, K., Rommel, C., Stocker, H. and Hafen, E. (2001). Ras controls growth, survival and differentiation in the Drosophila eye by different thresholds of MAP kinase activity. *Development* **128**, 1687-1696.
Harada, C., Nakamura, K., Namekata, K., Okumura, A., Mitamura, Y., Iizuka, Y., Kashiwagi, K., Yoshida, K., Ohno, S., Matsuzawa, A. et al. (2006). Role of apoptosis signal-regulating kinase 1 in stress-induced neural cell apoptosis in vivo. *Am. J. Pathol.* **168**, 261-269.
Hatakeyama, M. and Weinberg, R. A. (1995). The role of RB in cell cycle control. *Prog. Cell Cycle Res.* **1**, 9-19.
Henkemeyer, M., Orioli, D., Henderson, J. T., Saxton, T. M., Roder, J., Pawson, T. and Klein, R. (1996). Nuk controls pathfinding of commissural axons in the mammalian central nervous system. *Cell* **86**, 35-46.
Ho, C. Y. and Li, H. Y. (2010). DNA damage during mitosis invokes a JNK-mediated stress response that leads to cell death. *J. Cell Biochem.* **110**, 725-731.
Iaquinta, P. J. and Lees, J. A. (2007). Life and death decisions by the E2F transcription factors. *Curr. Opin. Cell Biol.* **19**, 649-657.
Jadhav, A. P., Roesch, K. and Cepko, C. L. (2009). Development and neurogenic potential of Muller glial cells in the vertebrate retina. *Prog. Retin. Eye Res.* **28**, 249-262.
Kimura, H., Spee, C., Sakamoto, T., Hinton, D. R., Ogura, Y., Tabata, Y., Ikada, Y. and Ryan, S. J. (1999). Cellular response in subretinal neovascularization induced by bFGF-impregnated microspheres. *Invest. Ophthalmol. Vis. Sci.* **40**, 524-528.
Labuda, T., Christensen, J. P., Rasmussen, S., Bonnesen, B., Karin, M., Thomsen, A. R. and Odum, N. (2006). MEK kinase 1 is a negative regulator of virus-specific CD8(+) T cells. *Eur. J. Immunol.* **36**, 2076-2084.
Levine, E. M., Close, J., Fero, M., Ostrovsky, A. and Reh, T. A. (2000). p27(Kip1) regulates cell cycle withdrawal of late multipotent progenitor cells in the mammalian retina. *Dev. Biol.* **219**, 299-314.
Li, Y., Minamino, T., Tsukamoto, O., Yujiri, T., Shintani, Y., Okada, K., Nagamachi, Y., Fujita, M., Hirata, A., Sanada, S. et al. (2005). Ablation of MEK kinase 1 suppresses intimal hyperplasia by impairing smooth muscle cell migration and urokinase plasminogen activator expression in a mouse blood-flow cessation model. *Circulation* **111**, 1672-1678.
Li, Z. Y., Possin, D. E. and Milam, A. H. (1995). Histopathology of bone spicule pigmentation in retinitis pigmentosa. *Ophthalmology* **102**, 805-816.
Lin, S. C., Skapek, S. X., Papermaster, D. S., Hankin, M. and Lee, E. Y. (2001). The proliferative and apoptotic activities of E2F1 in the mouse retina. *Oncogene* **20**, 7073-7084.
Livesey, F. J. and Cepko, C. L. (2001). Vertebrate neural cell-fate determination: lessons from the retina. *Nat. Rev. Neurosci.* **2**, 109-118.
MacPherson, D., Sage, J., Kim, T., Ho, D., McLaughlin, M. E. and Jacks, T. (2004). Cell type-specific effects of Rb deletion in the murine retina. *Genes Dev.* **18**, 1681-1694.
Menzel, N., Schneeberger, D. and Raabe, T. (2007). The Drosophila p21 activated kinase Mbt regulates the actin cytoskeleton and adherens junctions to control photoreceptor cell morphogenesis. *Mech. Dev.* **124**, 78-90.
Mihaly, J., Kockel, L., Gaengel, K., Weber, U., Bohmann, D. and Mlodzik, M. (2001). The role of the Drosophila TAK homologue dTAK during development. *Mech. Dev.* **102**, 67-79.
Mongan, M., Tan, Z., Chen, L., Peng, Z., Dietsch, M., Su, B., Leikauf, G. and Xia, Y. (2008). Mitogen-activated protein kinase kinase kinase 1 protects against nickel-induced acute lung injury. *Toxicol. Sci.* **104**, 405-411.
O'Driscoll, C., Donovan, M. and Cotter, T. G. (2006). Analysis of apoptotic and survival mediators in the early post-natal and mature retina. *Exp. Eye Res.* **83**, 1482-1492.
Oliveira, C. S., Rigon, A. P., Leal, R. B. and Rossi, F. M. (2008). The activation of ERK1/2 and p38 mitogen-activated protein kinases is dynamically regulated in the developing rat visual system. *Int. J. Dev. Neurosci.* **26**, 355-362.
Peng, Z., Peng, L., Fan, Y., Zandi, E., Shertzer, H. G. and Xia, Y. (2007). A critical role for IkappaB kinase beta in metallothionein-1 expression and protection against arsenic toxicity 1. *J. Biol. Chem.* **282**, 21487-21496.
Polager, S. and Ginsberg, D. (2009). p53 and E2f: partners in life and death. *Nat. Rev. Cancer* **9**, 738-748.
Reme, C. E., Grimm, C., Hafezi, F., Wenzel, A. and Williams, T. P. (2000). Apoptosis in the retina: the silent death of vision. *News Physiol. Sci.* **15**, 120-124.
Rowland, B. D. and Bernards, R. (2006). Re-evaluating cell-cycle regulation by E2Fs. *Cell* **127**, 871-874.
Schlesinger, T. K., Fanger, G. R., Yujiri, T. and Johnson, G. L. (1998). The TAO of MEKK. *Front. Biosci.* **3**, 1181-1186.
Sottocornola, R., Royer, C., Vives, V., Tordella, L., Zhong, S., Wang, Y., Ratnayaka, I., Shipman, M., Cheung, A., Gaston-Massuet, C. et al. (2010). ASPP2 binds Par-3 and controls the polarity and proliferation of neural progenitors during CNS development. *Dev. Cell* **19**, 126-137.
Stevaux, O. and Dyson, N. J. (2002). A revised picture of the E2F transcriptional network and RB function. *Curr. Opin. Cell Biol.* **14**, 684-691.
Takatori, A., Geh, E., Chen, L., Zhang, L., Meller, J. and Xia, Y. (2008). Differential transmission of MEKK1 morphogenetic signals by JNK1 and JNK2. *Development* **135**, 23-32.
Venuprasad, K., Elly, C., Gao, M., Salek-Ardakani, S., Harada, Y., Luo, J. L., Yang, C., Croft, M., Inoue, K., Karin, M. et al. (2006). Convergence of Itch-induced ubiquitination with MEKK1-JNK signaling in Th2 tolerance and airway inflammation. *J. Clin. Invest* **116**, 1117-1126.
Xia, Y. and Karin, M. (2004). The control of cell motility and epithelial morphogenesis by Jun kinases. *Trends Cell Biol.* **14**, 94-101.
Xia, Y., Makris, C., Su, B., Li, E., Yang, J., Nemerow, G. R. and Karin, M. (2000). MEK kinase 1 is critically required for c-Jun N-terminal kinase activation by proinflammatory stimuli and growth factor-induced cell migration. *Proc. Natl. Acad. Sci. USA* **97**, 5243-5248.
Yujiri, T., Sather, S., Fanger, G. R. and Johnson, G. L. (1998). Role of MEKK1 in cell survival and activation of JNK and ERK pathways defined by targeted gene disruption. *Science* **282**, 1911-1914.
Zhang, J., Gray, J., Wu, L., Leone, G., Rowan, S., Cepko, C. L., Zhu, X., Craft, C. M. and Dyer, M. A. (2004). Rb regulates proliferation and rod photoreceptor development in the mouse retina. *Nat. Genet.* **36**, 351-360.
Zhang, L., Wang, W., Hayashi, Y., Jester, J. V., Birk, D. E., Gao, M., Liu, C. Y., Kao, W. W., Karin, M. and Xia, Y. (2003). A role for MEK kinase 1 in TGF-beta/activin-induced epithelium movement and embryonic eyelid closure. *EMBO J.* **22**, 4443-4454.
Zhang, L., Deng, M., Parthasarathy, R., Wang, L., Mongan, M., Molkentin, J. D., Zheng, Y. and Xia, Y. (2005). MEKK1 transduces activin signals in keratinocytes to induce actin stress fiber formation and migration. *Mol. Cell. Biol.* **25**, 60-65.